

Performance Comparison of Various Substrates on a Wearable Ultra-Wideband Antenna

R. F. H. R. Idzhar¹, S. M. Shah^{1*}, H. A. Majid¹, U. Musa¹, N. S. Suriani²

¹ *Advanced Telecommunication Research Center (ATRC),
Universiti Tun Hussein Onn Malaysia, Parit Raja, Johor, 86400, MALAYSIA*

² *Faculty of Electrical and Electronic Engineering,
Universiti Tun Hussein Onn Malaysia, Parit Raja, Johor, 86400, MALAYSIA*

*Corresponding Author: shaharil@uthm.edu.my

DOI: <https://doi.org/10.30880/ijie.2024.16.01.019>

Article Info

Received: 17 November 2024

Accepted: 11 March 2024

Available online: 22 May 2024

Keywords

Ultra-wideband, microstrip antenna, bending investigation, substrate materials, wearable applications

Abstract

The substrate between the patch and ground plane of microstrip antenna plays an important role in antenna design as it dictates the linear characteristics performances of the antenna. This work focusses on the comparison between three UWB antennas fabricated on different substrate materials which are Rogers Duroid RO3003™ with a dielectric constant, ϵ_r of 3, loss tangent, $\tan \delta$ of 0.010 and thickness, h of 1.52 mm; denim substrate with ϵ_r of 1.7, $\tan \delta$ of 0.07 and h of 0.7 mm; and felt substrate with ϵ_r of 1.3, $\tan \delta$ of 0.02 and h of 1.1 mm. From the comparison, felt substrate offers a good antenna's performance in terms of frequency range, bandwidth, gain and efficiency followed by Rogers Duroid RO3003™ and denim substrates. The simulation results show that the frequency range of the UWB antenna with felt substrate is from 2.31 GHz to 11.74 GHz with a bandwidth of 9.43 GHz; gain, G of 5.489 dBi; and efficiency, η (%) of 91 %. The UWB antenna fabricated on RO3003™ has a frequency range from 2.94 GHz to 12.25 GHz with a bandwidth of 9.28 GHz, gain of 5.323 dBi and efficiency of 90%. Lastly, the antenna with denim substrate observed a frequency range from 2.67 GHz to 9.99 GHz with a bandwidth of 7.23 GHz, gain of 5.198 dBi and efficiency of 81.68%. The bending investigation are performed for each UWB antenna with different diameters ($d = 50$ mm, 80 mm and 100 mm) of vacuum cylinder in CST MWS® software and PVC pipes during measurement. It can be concluded from the simulated and measurement results that the performance of the antennas are not affected under bending condition and suitable to be worn on body for wearable applications.

1. Introduction

According to the Federal Communication Commission (FCC), ultra-wideband (UWB) signals emission is operated in between 3.1 GHz to 10.6 GHz [1]. The UWB system is widely used in applications such as medical sensing, military and indoor multipath wireless propagations [2]. An UWB antenna has the advantages of large bandwidth capacity, offers multipath propagation performance and has the potential for very-low-power implementation for transmitting-only devices [3]. A wearable antenna is known to be a part of the clothing used for communication purposes such as health monitoring, military purposes and security applications [4].

This is an open access article under the CC BY-NC-SA 4.0 license.



Wearable antennas are mostly fabricated on textile fabrics and due to that reason, they are commonly known as wearable textile antennas. One of the applications is to remotely monitor a patient's health condition which helps the doctor in diagnosing and controlling the diseases while working from home or clinic. In addition, a wearable antenna is meant to be a part of the apparel worn by human. This can be seen from the emergence of smart garments in various applications such as in medical diagnostics, sports, rescue workers military and space application [5].

The behavior of wearable antenna is mainly affected by the properties of the substrate materials [6]. For example, the efficiency and bandwidth of the antenna are affected by the thickness and relative permittivity (dielectric constant) of the substrates [7]. Therefore, the usage of textile or any substrate materials in a wearable antenna needs a classification in their properties in terms of the thickness, relative permittivity and loss tangent. The challenge in designing the antenna for wearable applications lies in the acceptability within the proximity of the human body and the effect of the radiation properties to human body in terms of Specific Absorption Rate (SAR). In order to protect the human body from excessive radiation, a standardized SAR limit which have been developed by the FCC and International Commission on Non-Ionizing Radiation Protection (ICNIRP) must be obeyed. The SAR limit regulated by the FCC is 1.6 W/kg when averaged over 1 g of human tissue and the SAR limit imposed by the ICNRP is 2 W/kg when averaged over 10 g of tissue [8]. Extensive investigation has been carried out into the development of various wearable substrates on UWB antennas from the past to present [9]. So, a question arises on which dielectric substrate among the common substrates available gives better performance and what are the properties of the dielectric substrates which affects the antenna performance. The substrate between the patch and ground plane of microstrip antenna plays an important role in antenna design as it dictates the bandwidth, size, gain and efficiency of that particular antenna [10]-[16]. Different substrates will have different dielectric constant, loss tangent and thickness. Extensive research on UWB antennas is driven by their numerous advantages, including large bandwidth, high data rates, low profile, compact size, light weight, low cost, stable radiation, security, and ease of fabrication [17]-[19]. These antennas exhibit omnidirectional radiation patterns and high gain. Recently, efforts have been focused on improving antenna properties by reducing their size [20]-[22].

In this work, a simple UWB antenna is designed and developed by using different substrate materials which are semi-flexible Rogers Duroid R03003™, flexible felt and denim fabrics. The purpose is to compare the performance of these antennas in terms of frequency range, bandwidth, reflection coefficient, gain and efficiency for wearable applications. The substrate between the patch and ground plane of microstrip antenna plays an important role in antenna design as it dictates the bandwidth, size, gain and efficiency of that particular antenna.

2. Methodology

In this section, the methodology employed to achieve the research results is elucidated, encompassing both the design and simulation stages conducted using CST MWS® software. The UWB antennas in this work are having the same geometry but with different dimensions. The dimensions are further optimized for each antenna with different substrates as one common dimensions might be the best for one antenna with a particular substrate but not for other substrates due to different substrate properties. The dielectric constant of denim and felt fabrics as substrate material are measured by using the Open-ended Dielectric Probe available at the Research Center for Applied Electromagnetics (EMCenter) while the thickness of each fabric is measured by using a micrometer. The work involves the design, presentation, and analysis of three UWB antennas on distinct substrates which are:

- i. UWB antenna with Rogers Duroid R03003™ substrate.
- ii. UWB antenna with denim substrate.
- iii. UWB antenna with felt substrate.

2.1 UWB Antenna with Rogers Duroid R03003™ Substrate

The proposed UWB antenna with rogers duroid substrate can be seen in Fig. 1 with top view and bottom view. The radiating patch at the top view is from copper material with a thickness of 0.035 mm. The substrate of this simulation antenna is using Rogers Duroid R03003™ with a dielectric constant, ϵ_r of 3, loss tangent, $\tan \delta$ of 0.010 and thickness, h of 1.52 mm. The ladder shape and a rectangular slot on the radiating patch are introduced to improve the impedance bandwidth of the antenna.

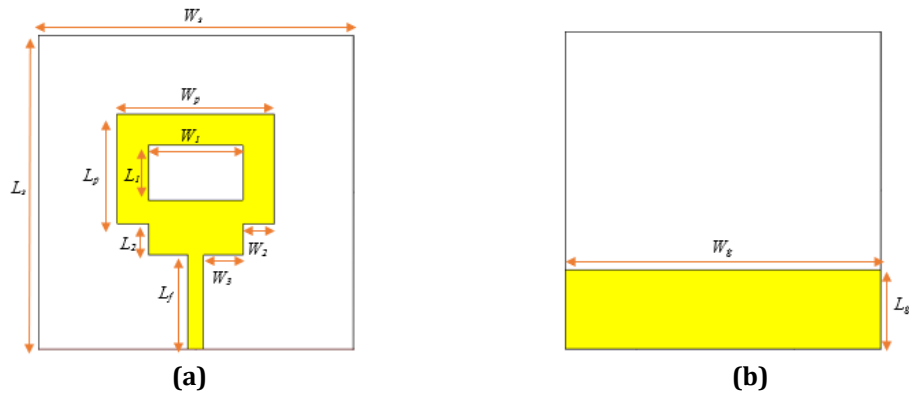


Fig. 1 The proposed UWB antenna with Rogers Duroid RO3003™ substrate (a) Top view; (b) Bottom view. The dimensions are $L_s = 40$ mm, $W_s = 40$ mm, $W_p = 20$ mm, $L_p = 14$ mm, $h = 1.52$ mm, $L_f = 12$ mm, $L_g = 10$ mm, $W_g = 40$ mm, $W_1 = 12$ mm, $L_1 = 7$ mm, $W_2 = 4$ mm, $L_2 = 4$ mm, $W_3 = 5$ mm

2.2 UWB Antenna with Denim Substrate

The proposed UWB antenna with denim substrate can be seen in Fig. 2 with top view and bottom view. The radiating patch at the top view is from copper material with a thickness of 0.035 mm. The substrate of this simulation antenna is using denim fabric with a dielectric constant, ϵ_r of 1.41, loss tangent, $\tan \delta$ of 0.07 and thickness, h of 0.7 mm. The ladder shape and a rectangular slot on the radiating patch are introduced to improve the impedance bandwidth of the antenna.

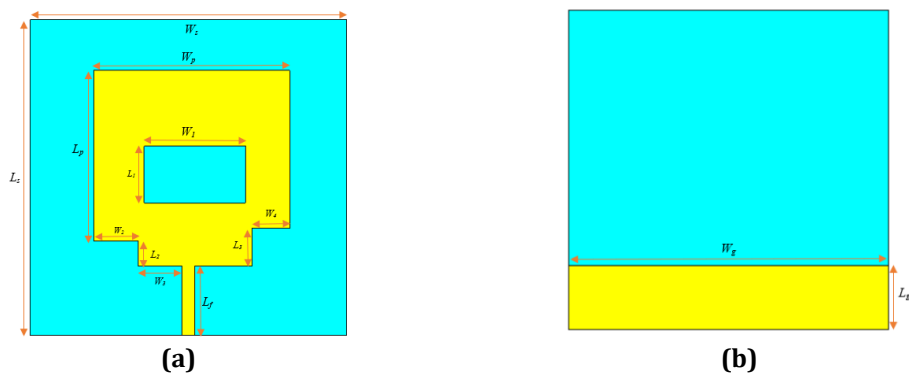


Fig. 2 The proposed UWB antenna with denim substrate (a) Top view; (b) Bottom view. The dimensions are $L_s = 50$ mm, $W_s = 50$ mm, $W_p = 31$ mm, $L_p = 25$ mm, $h = 0.7$ mm, $L_f = 11$ mm, $L_g = 10$ mm, $W_g = 50$ mm, $W_1 = 16$ mm, $L_1 = 9$ mm, $W_2 = 7$ mm, $L_2 = 4$ mm, $W_3 = 7$ mm, $W_4 = 6$ mm

2.3 UWB Antenna with Felt Substrate

The proposed UWB antenna with felt substrate can be seen in Fig. 3 with top view and bottom view. The radiating patch at the top view is from copper material with a thickness of 0.035 mm. The substrate of this simulation antenna is using felt fabric with a dielectric constant, ϵ_r of 1.2, loss tangent, $\tan \delta$ of 0.02 and thickness, h of 1.1 mm. The ladder shape and a rectangular slot on the radiating patch are introduced to improve the impedance bandwidth of the antenna.

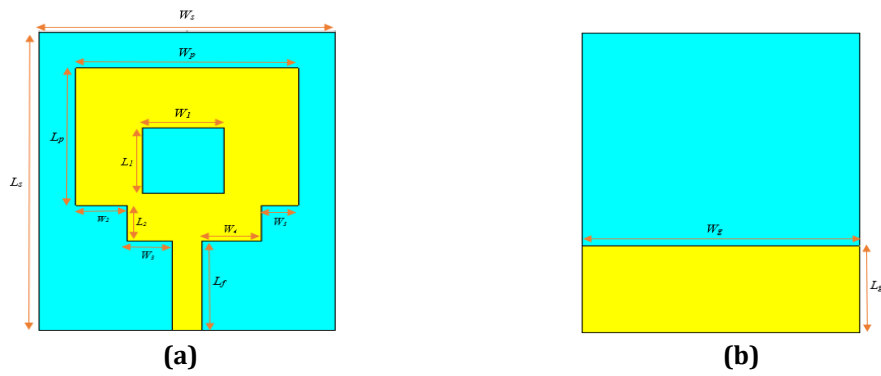


Fig. 3 The proposed UWB antenna with felt substrate (a) Top view; (b) Bottom view
 The dimensions are $L_s = 50$ mm, $W_s = 40$ mm, $W_p = 30$ mm, $L_p = 23$ mm, $h = 1.1$ mm, $L_f = 15$ mm, $L_g = 14.5$ mm, $W_g = 40$ mm, $W_1 = 14$ mm, $L_1 = 12$ mm, $W_2 = 7$ mm, $L_2 = 5$ mm, $W_3 = 6$ mm, $W_4 = 8$ mm, $W_5 = 5$ mm

3. Results and Analysis

In order to validate the design and simulations, the proposed antennas are fabricated, as shown in Fig. 4 (a)-(c). The N5234B Keysight Vector Network Analyzer (VNA) is employed to measure the antenna's reflection coefficient, as illustrated in Fig. 5.

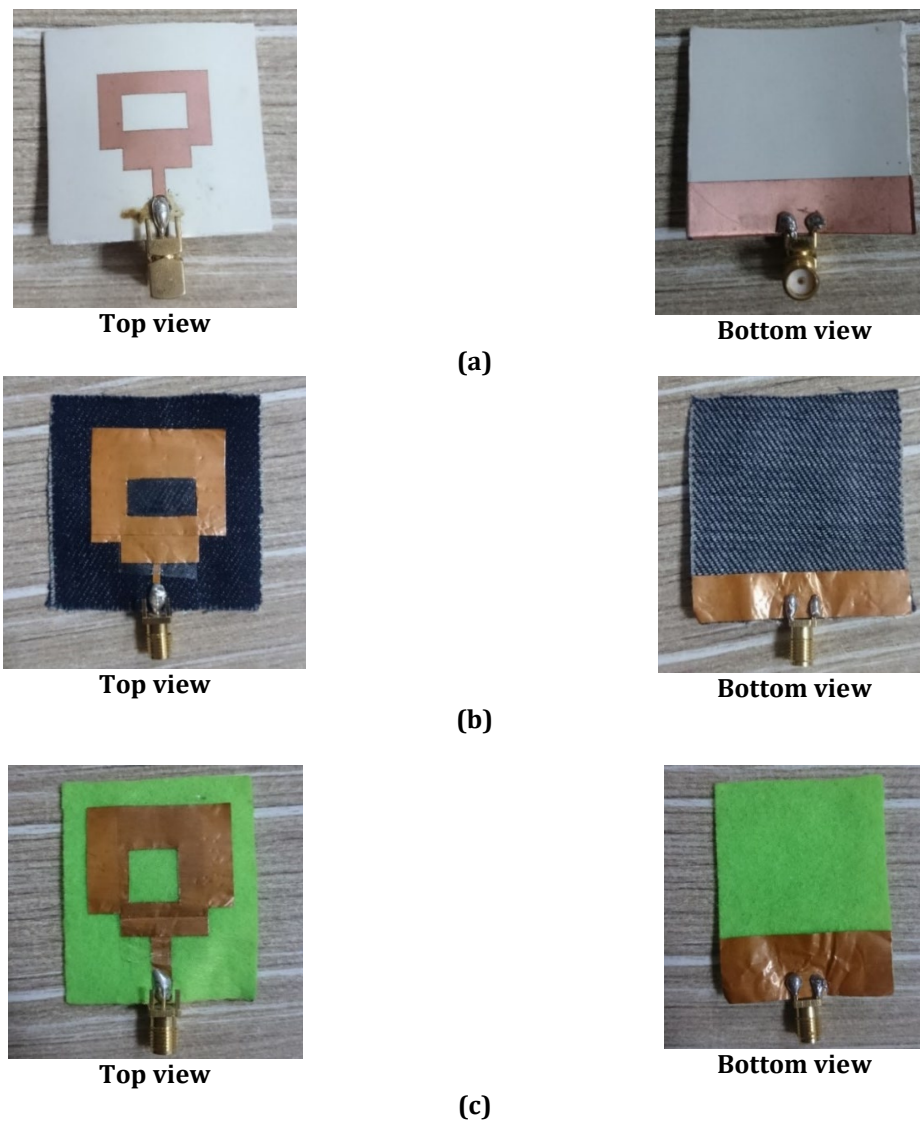


Fig. 4 Fabricated UWB antennas on (a) RO3003™ substrate; (b) Denim substrate; (c) Felt substrate

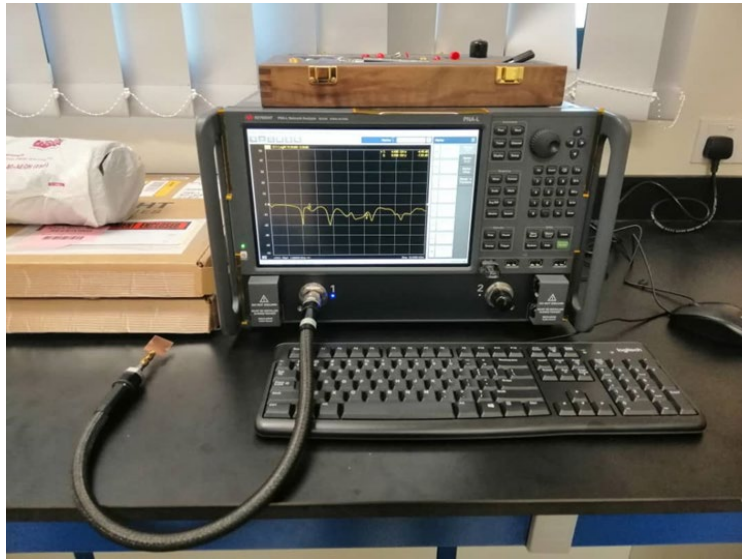


Fig. 5 Antenna's measurement using N5234B Keysight Vector Network Analyzer

3.1 Reflection Coefficient

This section compares the simulated and measured reflections coefficients of wearable UWB antennas with different substrate materials in this work.

3.1.1 UWB Antenna with Rogers Duroid R03003™ Substrate

Fig. 6 shows comparison between the simulated and measured reflection coefficients of UWB antenna with Rogers Duroid R03003™. From the figure, it can be observed that the antenna operates within the UWB frequency ranging from 2.09 GHz to 14.4 GHz with a bandwidth of 12.31 GHz. The difference between the measured and simulated reflection coefficients can be attributed to fabrication tolerance and cable losses.

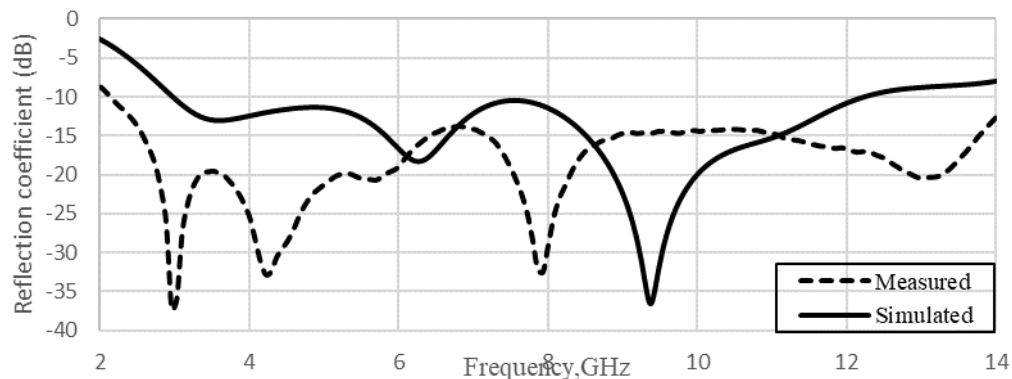


Fig. 6 Simulated and measured reflection coefficients of the UWB antenna with R03003™ substrate

3.1.2 UWB Antenna with Denim Substrate

Fig. 7 shows the comparison between the simulated and measured result of reflection coefficient of UWB antenna with denim substrate. From the figure, the frequency range of measured antenna is from 1.819 GHz to 4.930 GHz (bandwidth of 3.11 GHz) and 5.75 to 10.83 GHz (bandwidth of 5.08).

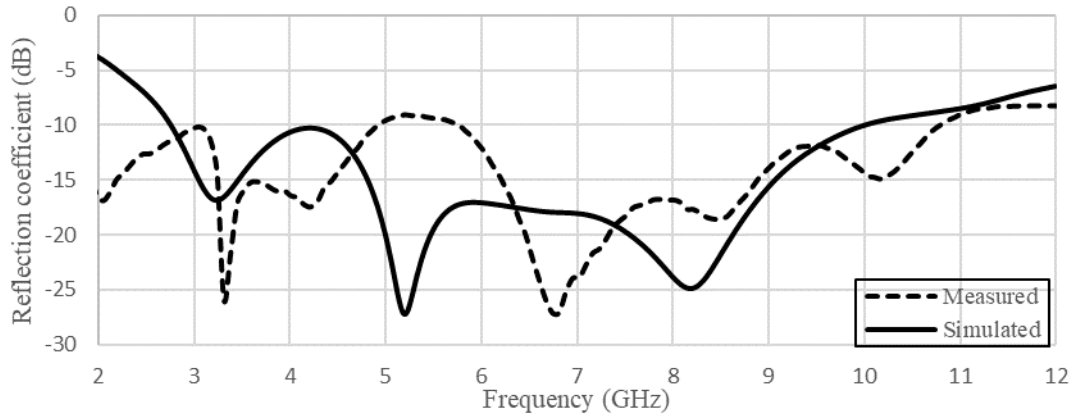


Fig. 7 Simulated and measured reflection coefficients of the UWB antenna with denim substrate

3.1.3 UWB Antenna with Felt Substrate

Fig. 8 shows the comparison between simulated and measured result of reflection coefficient of UWB antenna with felt substrate. From the figure, the measured reflection coefficient has a frequency range from 1.91 GHz to 9.61 GHz (bandwidth of 7.7 GHz) while. The difference between the measured and simulation can be attributed to fabrication tolerance and cable losses.

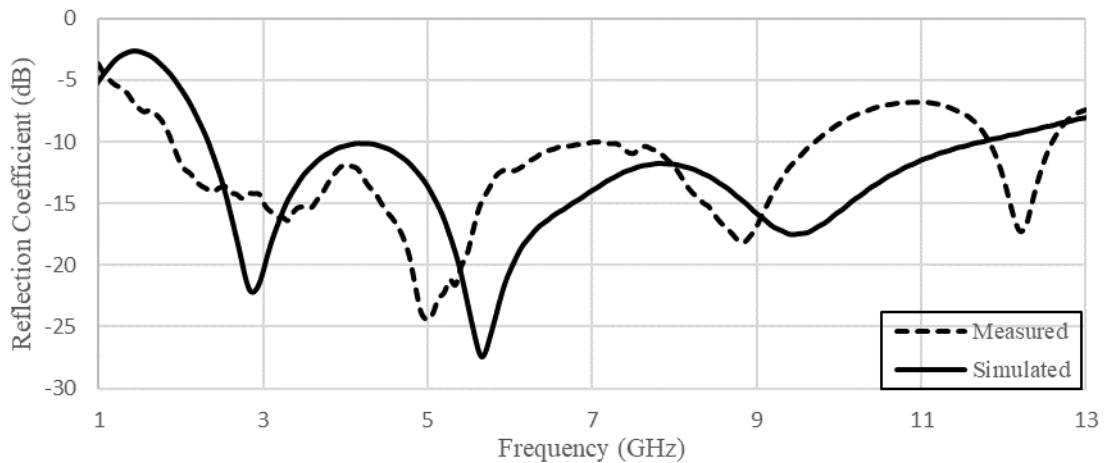


Fig. 8 Simulated and measured reflection coefficients of the UWB antenna with felt substrate

3.2 Surface Current Distribution

The surface current distributions of the UWB antenna with Rogers Duroid RO3003™ at 2.97 GHz, 7.67 GHz and 12.25 GHz are simulated in CST MWS® software and can be viewed in Fig. 9. From Fig. 9 (a), the maximum current is seen to be concentrated around the edges of the feed line at 2.97 GHz. From Fig.9 (b), the maximum current is seen to be concentrated around the edges of the feed line and around top edge of the partial ground plane and bottom edge of the radiating patch at 7.67 GHz. A small area of maximum current can also be seen around the edges of the rectangular slot. Last but not least, the maximum current in Fig.9 (c) is seen to be concentrated around the edges of the feed line and also around the top edges of the partial ground plane at 12.25 GHz.

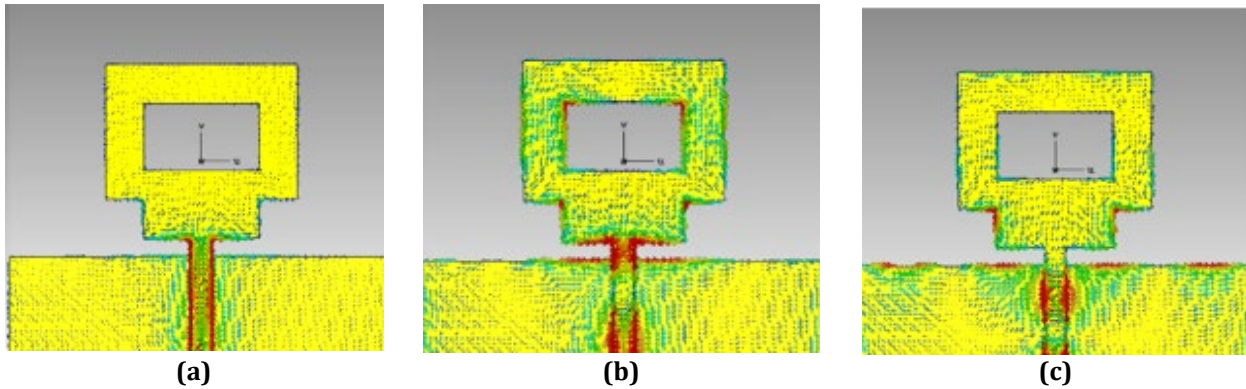


Fig. 9 Surface current distribution of the UWB antenna with RO3003™ substrate
(a) 2.97 GHz; (b) 7.67 GHz; (c) 12.25 GHz

The surface current distributions of the UWB antenna with denim substrate at 2.28 GHz, 6.37 GHz and 9.99 GHz can be viewed in Fig. 10. From Fig. 10 (a), the maximum current is seen to be concentrated around the edges of feed line at 2.28 GHz. From Fig. 10 (b), the maximum current is seen to be concentrated around the edges of the feed line and around the bottom edges of the square patch at 6.37 GHz. Last but not least, the maximum current from Fig. 10 (c) is seen to be concentrated around the edges of the feed line, around the bottom edges of the radiating patch and mostly around the top edges of partial ground plane at 9.99 GHz.

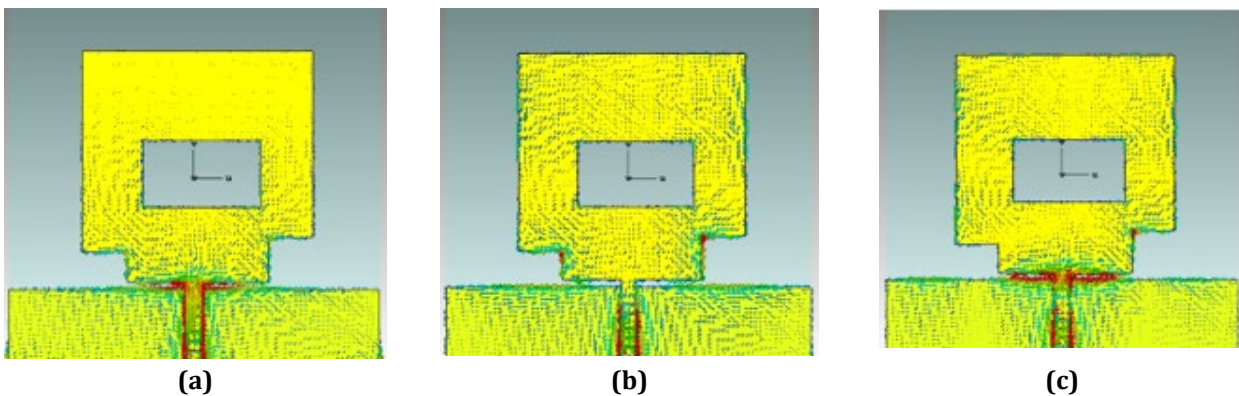


Fig. 10 Surface current distribution of the UWB antenna with denim substrate
(a) 2.28 GHz; (b) 6.37 GHz; (c) 9.99 GHz

The surface current distributions of the UWB antenna with felt substrate at 2.31 GHz, 7.02 GHz and 11.74 GHz can be observed in Fig. 11. From Fig. 11 (a), the maximum current is seen to be concentrated around the edges of feed line and at the bottom edges of the radiating patch at 2.31 GHz. From Fig. 11 (b), the maximum current is seen to be concentrated around the edges of the feed line and at the bottom edges of the square patch at 7.02 GHz. Last but not least, the maximum current from Fig. 11 (c) is seen to be concentrated around the top edges and at the bottom edges of the feed line at 11.74 GHz. A small area of maximum current can also be seen around the edges of the rectangular slot.

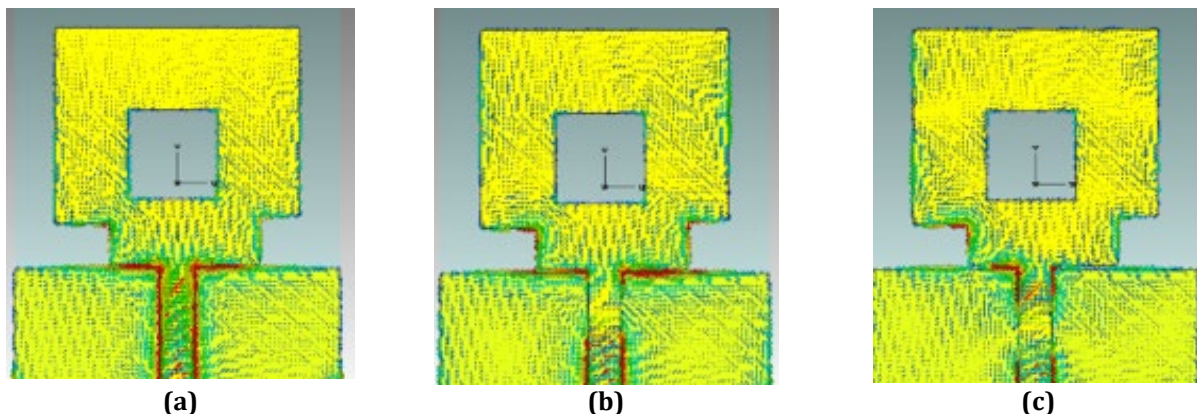


Fig. 11 Surface current distribution of the UWB antenna with felt substrate:
(a) 2.31 GHz; (b) 7.02 GHz; (c) 11.74 GHz

3.3 Radiation Pattern, Gain and Efficiency

The 2D and 3D far-field radiation patterns in the *E*-plane of the antenna with Rogers Duroid RO3003™ are simulated at 2.97 GHz, 7.67 GHz and 12.25 GHz which are shown in Fig. 12. From Fig. 12 (a), the antenna has a bi-directional radiation pattern with a doughnut-shaped pattern. Nevertheless, the radiation patterns slightly deteriorate at higher frequencies by producing nulls in certain directions as seen from Fig. 12 (b) and (c), but still meets the requirements of UWB communication system. The simulated gain, *G* of the antenna at those chosen frequencies are 2.454 dBi, 5.148 dBi and 5.862 dBi while the efficiency, η (%) are calculated at 86.2%, 84.48%, and 82.43%, respectively.

Omni-directional radiation patterns are observed in the *H*-plane of all antennas at the same frequencies as in the *E*-plane. Due to limitation on the number of pages, the results are not presented.

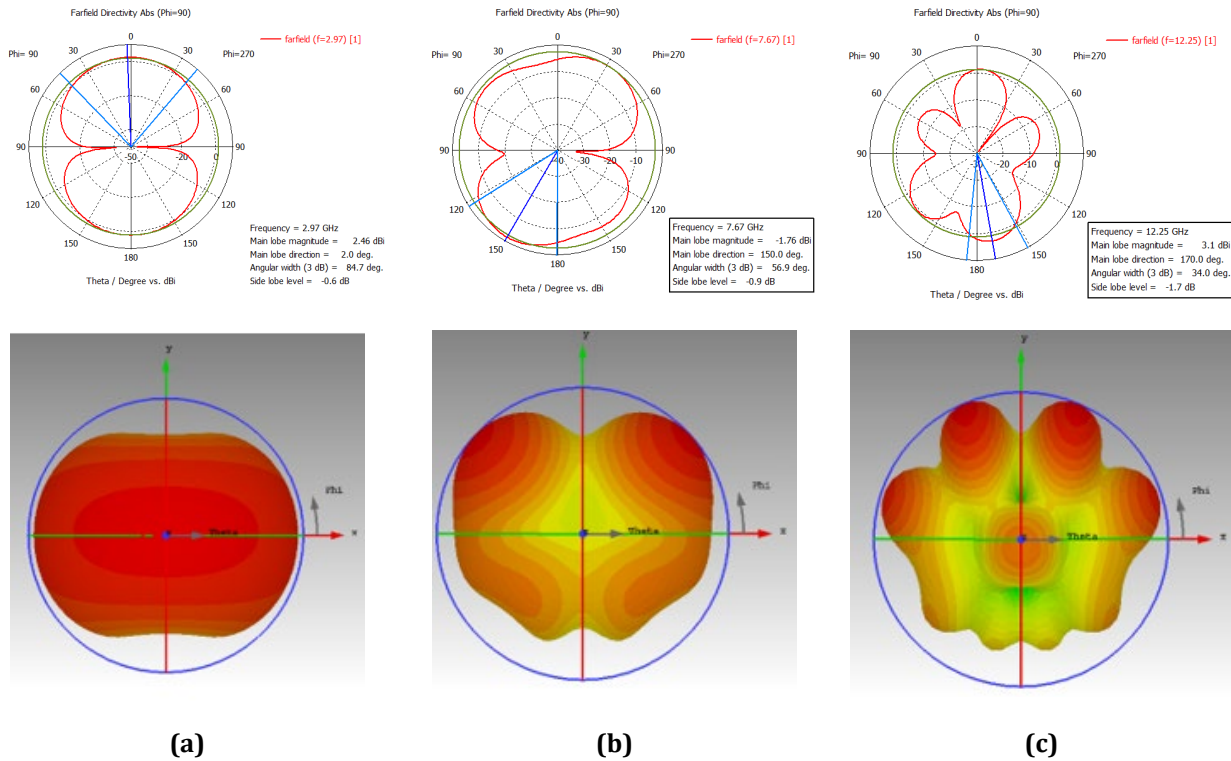
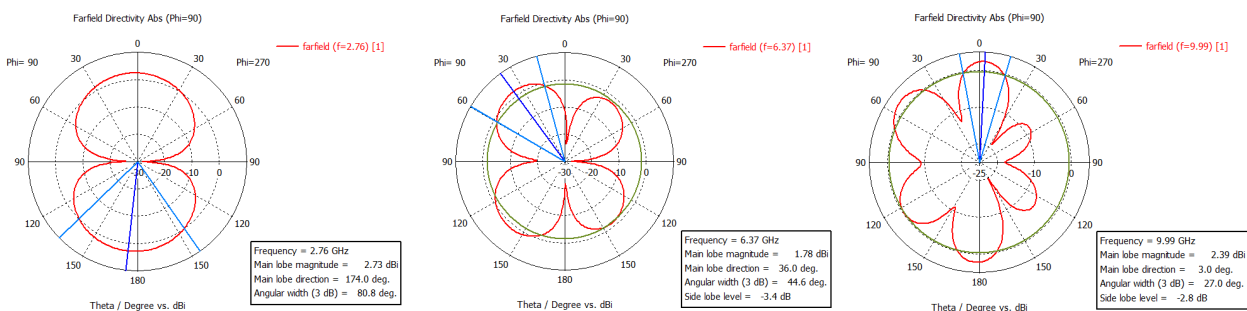


Fig. 12 2D and 3D radiation patterns in the *E*-plane of the UWB antenna with RO3003™ substrate at frequency (a) 2.97 GHz; (b) 7.67 GHz; (c) 12.25 GHz

Next, the 2D and 3D radiation patterns in the *E*-plane of the antenna with denim substrate are simulated at 2.76 GHz, 6.37 GHz and 9.99 GHz, as can be viewed in Fig. 13. Similarly, the antenna has a bi-directional radiation pattern with a doughnut-shaped pattern as seen from Fig. 13 (a). From Fig. 13 (b) and (c), the radiation patterns slightly deteriorate at higher frequencies. The simulated gain, *G* of the antenna at those frequencies are 2.734 dBi, 5.275 dBi and 5.090 dBi. The efficiency, η (%) can then be calculated at 86%, 84% and 74%, respectively.

Omni-directional radiation patterns are observed in the *H*-plane of all antennas at the same frequencies as in the *E*-plane. Due to limitation on the number of pages, the results are not presented.



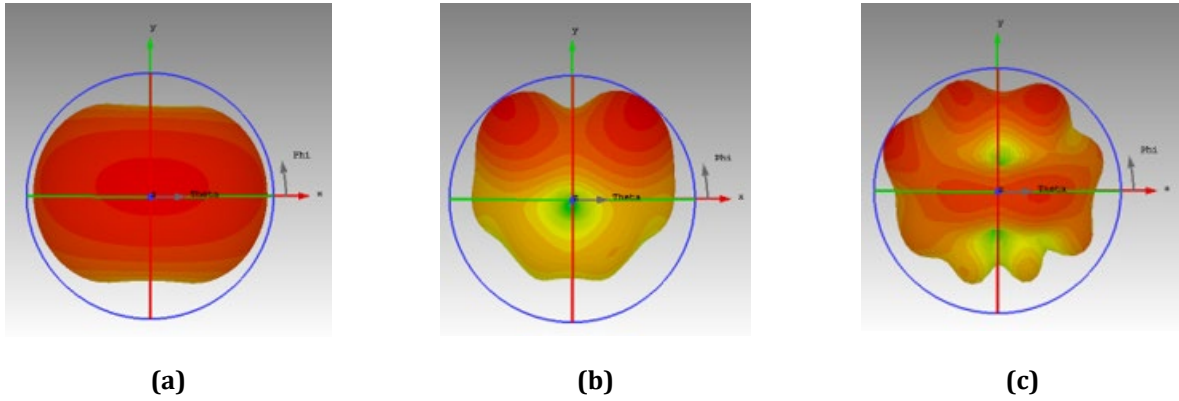


Fig. 13 2D and 3D radiation patterns the *E*-plane of the UWB antenna with denim substrate at frequency (a) 2.76 GHz; (b) 6.37 GHz; (c) 9.99 GHz

Finally, the 2D and 3D radiation patterns in the *E*-plane of the antenna with felt substrate are simulated at 2.31 GHz, 7.02 GHz and 11.74 GHz as can be seen in Fig. 14. Similarly, the proposed antenna has a bi-directional radiation pattern with a doughnut-shaped pattern as shown from Fig. 14 (a). However, from Fig. 14 (b) and (c), the radiation patterns slightly deteriorate at higher frequencies. The simulated gain, G of the antenna at 2.31 GHz, 7.02 GHz and 11.74 GHz are 2.529 dBi, 4.335 dBi and 5.179 dBi while the efficiency, $\eta(\%)$ are calculated 90.4%, 84.48% and 85.6%.

Omni-directional radiation patterns are observed in the *H*-plane of all antennas at the same frequencies as in the *E*-plane. Due to limitation on the number of pages, the results are not presented.

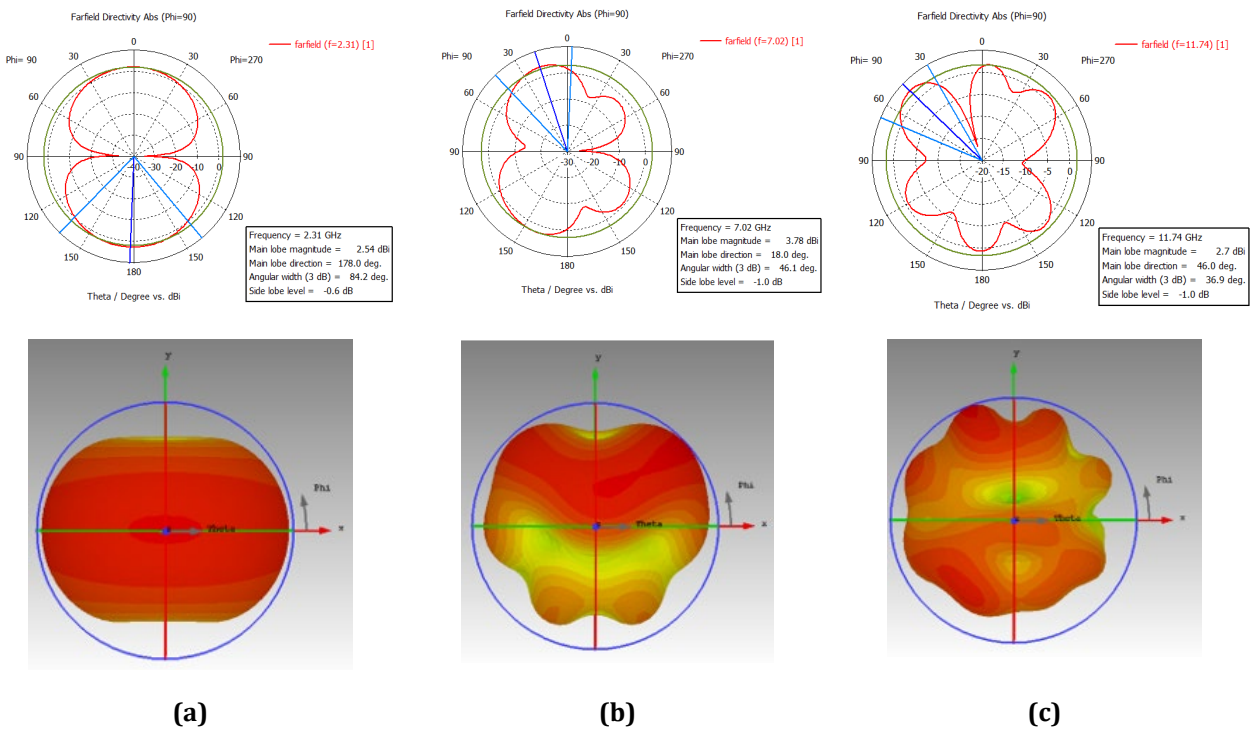


Fig. 14 2D and 3D radiation patterns the *E*-plane of the UWB antenna with felt substrate at frequency (a) 2.31 GHz; (b) 7.02 GHz; (c) 11.74 GHz

3.4 Bending Investigation

The bending investigation is performed along *y*-axis in CST MWS® software to simulate the reflection coefficient of the antenna on a vacuum cylinder with varying diameters, d of 50 mm, 80 mm and 100 mm. The diameters are selected according to the average human arm sizes. PVC pipes with diameter of 50 mm, 80 mm and 100 mm

are used for measurement of bending condition. The PVC pipes is selected due to its similarity with the human arm. The fabricated UWB antenna are attached to the PVC pipe as shown in Fig. 15.

Fig. 16 shows the comparison of simulated and measured reflection coefficients of the antenna with RO3003™ substrate under bending condition for all diameters of PVC pipes. From Fig. 16 (a), the simulated reflection coefficients of the antenna for all diameters are almost similar. From Fig. 16 (b), it can be observed that the simulated reflection coefficients are almost similar except for $d = 50$ mm. However, the UWB frequency range are still covered for all diameters which show that the antenna operates well within the frequency band and suitable for wearable applications.

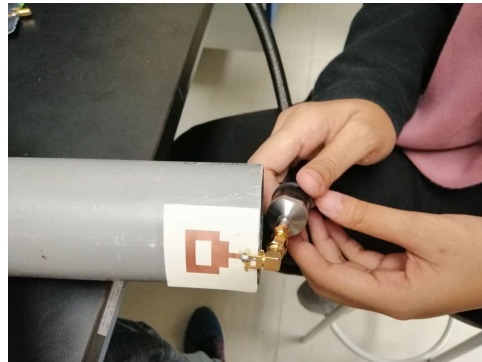


Fig. 15 The measurement of the UWB antenna on bending condition using different diameters of PVC pipes

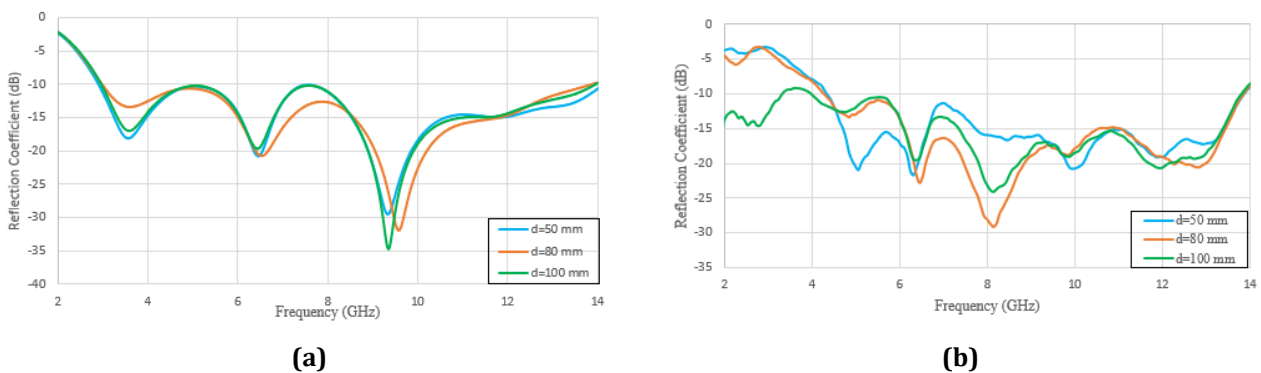


Fig. 16 Reflection coefficient for different bending diameters of the UWB antenna with RO3003™ substrate
(a) Simulated; (b) Measured

Similarly, Fig. 17 shows the comparison of simulated and measured reflection coefficients of the antenna, but with denim substrate. From Fig. 17 (a), the simulated reflection coefficients for 50-mm and 80-mm diameters are almost similar. However, the reflection coefficient for 100-mm diameter deviates significantly but it is still greater than the -10-dB line. These imply that the performance of the antenna is not affected regardless of the variation in PVC pipe diameters. Fig. 17 (b) shows the measured reflection coefficients of the antenna. From the figure, it can be observed that the reflection coefficients are in a good agreement for all diameters. Therefore, the performance of the UWB antenna is not affected under different bending conditions and serves as a good candidate for wearable applications.

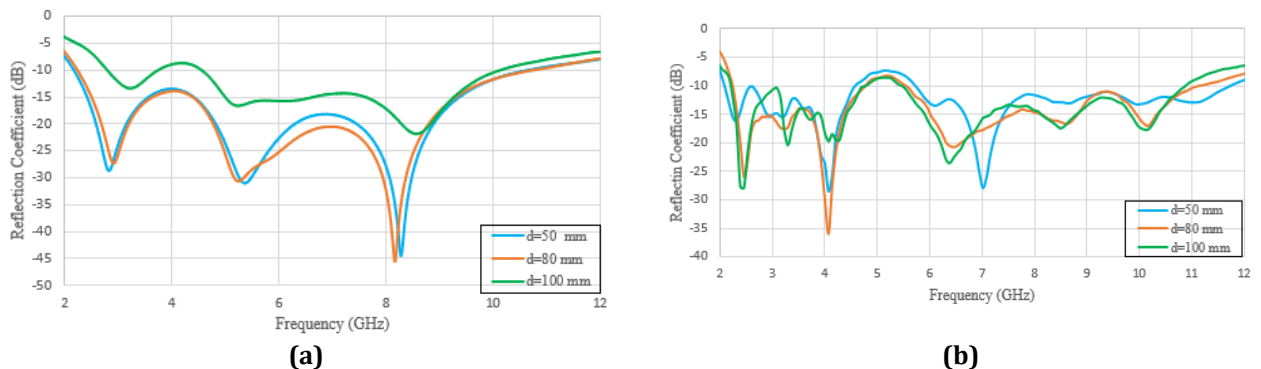


Fig. 17 Reflection coefficient for different bending diameters of the UWB antenna with denim substrate (a) Simulated; (b) Measured

Fig. 18 shows the comparison of simulated and measured reflection coefficients of the antenna, but with felt substrate. From Fig. 18 (a), the reflection coefficients of the antenna are almost similar, which imply that the performance of antenna is not affected under bending condition. The measured reflection coefficients are shown in Fig. 18 (b). From the figure, it can be deduced that the reflection coefficients are almost identical for all diameters of PVC pipe. Therefore, it can be concluded that the performance of antenna under different bending conditions are not affected which makes it comfortable to be worn on body for wearable applications.

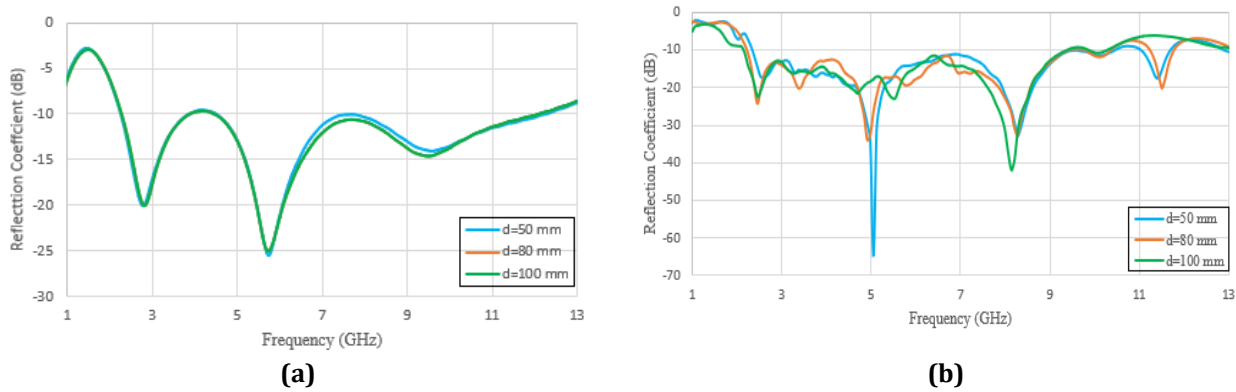


Fig. 18 Reflection coefficient for different bending diameters of the UWB antenna with felt substrate (a) Simulated; (b) Measured

Table 1 lists all the performance comparison of all UWB antennas in this work with different substrate materials namely, RO3003™, denim and felt. From the three, RO3003™ is a semi-flexible substrate whereas denim and felt are flexible fabric substrates. From the table, the UWB antenna with felt substrate has the widest frequency range from 2.31 GHz to 11.74 GHz with a bandwidth of 9.43 GHz followed by RO3003™ and denim substrates. In terms of gain and efficiency, the UWB antenna with felt substrate has the highest gain and efficiency of 5.489 dBi and 91%, respectively. This is followed by RO3003™ and denim substrate. Thus, from the comparison, the order of substrates performances is consistent for each linear characteristic. Therefore, it can be concluded that the UWB antenna with felt substrate offers better performance as compared to UWB antennas with RO3003™ and denim substrates.

Table 1 Comparison between three different substrates on an UWB antenna

	Substrate Materials		
	RO3003™	Denim Fabric	Felt Fabric
UWB Antenna			
Substrates Properties	$\epsilon_r = 3,$ $\tan \delta = 0.010$ $h = 1.52 \text{ mm}.$	$\epsilon_r = 1.41$ $\tan \delta = 0.07$ $h = 0.7 \text{ mm}.$	$\epsilon_r = 1.2$ $\tan \delta = 0.02$ $h = 1.1 \text{ mm}.$

UWB Frequency Range	2.97 GHz to 12.25 GHz	2.76 GHz to 9.99 GHz	2.31 GHz to 11.74 GHz
Bandwidth	9.28 GHz	7.23 GHz	9.43 GHz
Frequency at Greatest Reflection Coefficient	9.38 GHz	5.20 GHz	5.65 GHz
Gain	5.323 dBi	5.198 dBi	5.489 dBi
Efficiency	90.7%	81.68%	91%

4. Conclusion

In this work, three UWB antennas with Rogers Duroid RO3003™, denim and felt substrates have been designed, simulated and fabricated. The performance comparison between the antennas is then performed in terms of their linear characteristics which consist of frequency range, bandwidth, gain and efficiency. From the comparison, it can be concluded that the UWB antenna with felt substrate offers better performance as compared to UWB antennas with RO3003™ and denim substrates. This can be deduced from the fact that the UWB antenna with felt substrate has the widest frequency range from 2.31 GHz to 11.74 GHz with a bandwidth of 9.43 GHz followed by RO3003™ and denim substrates. In terms of gain and efficiency, the UWB antenna with felt substrate has the highest gain and efficiency of 5.489 dBi and 91%, respectively. This is followed by RO3003™ and denim substrate. The bending investigation is performed for each UWB antenna on different diameters ($d = 50$ mm, 80 mm and 100 mm) of vacuum cylinder in CST MWS® software and PVC pipes during the measurement. From the comparison between the simulated and measured reflection coefficients the UWB frequency range is still observed regardless of the diameters. Therefore, it can be concluded that the performance of the UWB antennas are not compromised under bending condition and suitable to be worn on body for wearable applications.

Acknowledgement

This work was supported by the Ministry of Higher Education (MoHE) under Fundamental Research Grant Scheme FRGS/1/2020/TK0/UTHM/02/44.

Conflict of Interest

Authors declare that there is no conflict of interests regarding the publication of the paper.

Author Contribution

The authors confirm contribution to the paper as follows: **study conception and design:** R. F. H. R. Idzhar, S. M. Shah; **data collection:** R. F. H. R. Idzhar; **analysis and interpretation of results:** R. F. H. R. Idzhar; **draft manuscript preparation:** S. M. Shah, H. A. Majid, U. Musa, N. S. Suriani. All authors reviewed the results and approved the final version of the manuscript.

References

- [1] Chan, K., Chia, M., Leong, S. W., & Sim, C. K. (2005). *Through-wall UWB radar operating within FCC mask for sensing heart beat and breathing rate*. <https://doi.org/10.1109/EURAD.2005.1605615>.
- [2] Fayadh, R., AbdulMalek, M., Fadhil, H., & Saudin, N. (2013). Design of ultra wideband rectangular microstrip notched patch antenna. *Proceedings - 2013 IEEE International Conference on Control System, Computing and Engineering, ICCSCE 2013*, 408–412. <https://doi.org/10.1109/ICCSCE.2013.6719999>.
- [3] Jiang, Z., & Werner, D. (2015). A Compact, Wideband Circularly Polarized Co-designed Filtering Antenna and Its Application for Wearable Devices With Low SAR. *Antennas and Propagation, IEEE Transactions On*, 63, 3808–3818. <https://doi.org/10.1109/TAP.2015.2452942>.
- [4] Kalteh, A., Nikmeh, S., & Eskandarnejad, A. (2013). Directional UWB Microstrip Antenna for Radar Applications. *International Journal of Basic Sciences & Applied Research*, 133-138. <https://api.semanticscholar.org/CorpusID:27557113>.

- [5] Kishk, A. A., Zunoubi, M. R., & Kajfez, D. (1993). A numerical study of a dielectric disk antenna above grounded dielectric substrate. *IEEE Transactions on Antennas and Propagation*, 41(6), 813–821. <https://doi.org/10.1109/8.250458>.
- [6] Lim, E., Wang, Z., Wang, J., Leach, M., Zhou, R., Lei, C.-U., & Man, K. (2014). Wearable Textile Substrate Patch Antennas. *Engineering Letters*, 22, 94–101.
- [7] Salvado, R., Loss, C., Gonçalves, R., & Pinho, P. (2012). Textile Materials for the Design of Wearable Antennas: A Survey. *Sensors*, 12(11), 15841–15857. <https://doi.org/10.3390/s121115841>.
- [8] Singh, N., Singh, A. K., & Singh, V. K. (2015). Design and performance of wearable ultrawide band textile antenna for medical applications. *Microwave and Optical Technology Letters*, 57(7), 1553–1557. <https://doi.org/https://doi.org/10.1002/mop.29131>.
- [9] Tsolis, A., Whittow, W. G., Alexandridis, A. A., & Vardaxoglou, J. C. (2014). Embroidery and Related Manufacturing Techniques for Wearable Antennas: Challenges and Opportunities. *Electronics*, 3(2), 314–338. <https://doi.org/10.3390/electronics3020314>.
- [10] Wiri, A. T. (2021). Novel Stitched Ground Plane Optimizations for Microstrip Patch Antennas at Wi-Fi and WiMAX Applications. *Open Journal of Antennas and Propagation*, 09. <https://doi.org/10.4236/ojapr.2021.92003>.
- [11] F. Xu, X. Chen, and X.-A. Wang, "UWB antenna with triple notched bands based on folded multiple-mode resonators," *IEICE Electron. Express*, vol. 9, pp. 965–970, 2012, doi: 10.1587/elex.9.965.
- [12] Sarkar, D., Srivastava, K. V., & Saurav, K. (2014). A Compact Microstrip-Fed Triple Band-Notched UWB Monopole Antenna. *IEEE Antennas and Wireless Propagation Letters*, 13, 396–399. <https://doi.org/10.1109/LAWP.2014.2306812>.
- [13] Balani, W., Sarvagya, M., Ali, T., Samasgikar, A., Das, S., Kumar, P., & Anguera, J. (2021). Design of SWB Antenna with Triple Band Notch Characteristics for Multipurpose Wireless Applications. *Applied Sciences*, 11(2). <https://doi.org/10.3390/app11020711>.
- [14] Kumar, G., & Kumar, R. (2019). A Survey on Planar Ultra-Wideband Antennas with Band notch Characteristics: Principle, Design, and Applications. *AEU - International Journal of Electronics and Communications*, 109, 76–98. <https://doi.org/10.1016/j.aeue.2019.07.004>.
- [15] Sanyal, R., Sarkar, P., & Sarkar, S. (2019). Octagonal nut shaped monopole UWB antenna with sextuple band notched characteristics. *AEU - International Journal of Electronics and Communications*, 110, 152833. <https://doi.org/10.1016/j.aeue.2019.152833>.
- [16] Musa, U., Shah, S. M., Majid, H. A., Mahadi, I. A., Rahim, M. K. A., Yahya, M. S., & Abidin, Z. Z. (2023). Design and Analysis of a Compact Dual-Band Wearable Antenna for WBAN Applications. *IEEE Access*, 11, 30996–31009. <https://doi.org/10.1109/ACCESS.2023.3262298>.
- [17] Yalduz, H., Tabaru, T. E., Kilic, V. T., & Turkmen, M. (2020). Design and analysis of low profile and low SAR full-textile UWB wearable antenna with metamaterial for WBAN applications. *AEU - International Journal of Electronics and Communications*, 126, 153465. <https://doi.org/https://doi.org/10.1016/j.aeue.2020.153465>.
- [18] Yan, S., Poffelie, L. A. Y., Soh, P. J., Zheng, X., & Vandenbosch, G. A. E. (2016). On-body performance of wearable UWB textile antenna with full ground plane. 2016 10th European Conference on Antennas and Propagation (EuCAP), 1–4. <https://doi.org/10.1109/EuCAP.2016.7481477>.
- [19] Kumari, A., Badhai, R., & Suraj, P. (2018). A Compact Polygon Shape Ultra Wideband Antenna For Portable Devices. 1–4. <https://doi.org/10.1109/WiSPNET.2018.8538728>.
- [20] Sharma, P., & Vaish, A. (2018). Developments In Ultrawideband(UWB) Antennas. 380–385. <https://doi.org/10.1109/ICCMC.2018.8487698>.
- [21] Park, S., & Jung, K.-Y. (2022). Novel Compact UWB Planar Monopole Antenna Using a Ribbon-Shaped Slot. *IEEE Access*, 10, 61951–61959. <https://doi.org/10.1109/ACCESS.2022.3182443>.
- [22] Schantz, H. (2003). Introduction to ultra-wideband antennas. *IEEE Conf Ultra-Wideband Syst and Technologies*, 1–9. <https://doi.org/10.1109/UWBST.2003.1267792>.